Proceedings of HT2005
2005 ASME Summer Heat Transfer Conference
July 17-22, 2005, San Francisco, California, USA

HT2005-72651

CRYOGENIC CHILLDOWN MODEL FOR STRATIFIED FLOW INSIDE A PIPE

Jun Liao **Kun Yuan**

Renwei Mei **James F. Klausner** **Jacob Chung**

Department of Mechanical and Aerospace Engineering, University of Florida, Gainesville, FL 32611, USA

ABSTRACT

A pseudo-steady model has been developed to predict the chilldown history of the pipe wall temperature in horizontal transport pipelines for cryogenic fluids. A new film boiling heat transfer model is developed by incorporating the stratified flow structure for cryogenic chilldown. A modified nucleate boiling heat transfer correlation for the cryogenic chilldown process inside a horizontal pipe is proposed. The efficacy of the correlations is assessed by comparing the model predictions with measured values of wall temperature in several azimuthal positions in a well controlled experiment by Chung et al. (2004). The computed pipe wall temperature histories match well with the measured results. The present model captures important features of thermal interaction between the pipe wall and the cryogenic fluid, provides a simple and robust platform for predicting the pipe wall chilldown history in a long horizontal pipe at relatively low computational cost, and builds a foundation to incorporate the two-phase hydrodynamic interaction in the chilldown process.

INTRODUCTION

Cryogenic chilldown is encountered in many applications but is of particular importance in cryogenic transportation pipelines. For example, in rockets or space shuttle launch facilities, cryogenic propellants fill the internal fuel tanks of a space vehicle through a complex pipeline system. To avoid evaporated fuel entering the space vehicle, a cryogenic chilldown prior to the filling is required to reduce the pipe wall temperature to the saturation temperature of the cryogenic liquid.

Cryogenic chilldown involves complicated hydrodynamic and thermal interactions among the liquid, the vapor, and the solid pipe wall. There exist a few basic experimental studies and modeling efforts for chilldown of cryogenic fluids. Studies on cryogenic chilldown started in the 1960's accompanying the development of rocket launching systems. Early experimental studies were conducted by Burke et al. [1], Graham [2], Bronson et al. [3], Chi and Vetere [4], Steward [5] among other researches. Bronson et al. [3] studied flow regimes in a horizontal pipe during chilldown with liquid hydrogen. The results revealed that stratified flow is prevalent during cryogenic chilldown.

Flow regimes and heat transfer regimes in a horizontal pipe during cryogenic chilldown were also studied by Chi and Vetere [4]. Information on flow regimes was deduced by studying the fluid temperature and the volume fraction during chilldown. Several flow regimes were identified: single phase vapor, mist flow, slug flow, annular flow, bubbly flow, and single-phase liquid flow. Heat transfer regimes were identified as: single-phase vapor convection, film boiling, nucleate boiling, and single-phase liquid convection.

Recently, Velat et al. [6] systematically studied cryogenic chilldown with nitrogen in a horizontal pipe. Their study included: a visual recording the chilldown process in a transparent Pyrex pipe, which is used to identify the flow regime and heat transfer regime; collecting temperature histories at different positions of the wall in chilldown; and recording the pressure drop along the pipe. Chung et al. [7] conducted a similar study with nitrogen chilldown at relatively low mass flux and provided the data needed to assess various heat transfer coefficients in the present study.

Burke et al. [1] developed a crude chilldown model based on one-dimensional heat transfer through the pipe wall and the assumption of infinite heat transfer rate from the cryogenic fluid to the pipe wall. The effects of flow regimes on the heat transfer rate were neglected. Graham et al. [2] correlated heat transfer coefficient and pressure drop with the Martinelli number [8] based on their experimental data. Chi [9] developed a one-dimensional model for energy equations of the liquid and the wall, based on the film boiling heat transfer between the wall and fluid. An empirical equation for predicting chilldown time and temperature was proposed.

Steward [5] developed a homogeneous flow model for cryogenic chilldown. The model treated the cryogenic fluid as a

homogeneous mixture. The continuity, momentum and energy equations of the mixture were solved to obtain density, pressure and temperature of mixture. Various heat transfer regimes were considered: film boiling, nucleate boiling and single-phase convection heat transfer. Separate treatment of different heat transfer regimes resulted in a significant improvement in the prediction of the chilldown time. The homogeneous mixture model was also employed by Cross et al. [10] who obtained a correlation for the wall temperature during chilldown with an oversimplified treatment of the heat transfer between the wall and the fluid.

The stratified flow regime, which is the prevalent flow regime in the horizontal chilldown, was first studied by Chen and Banerjee [11-13]. They developed a separated flow model for the simulating the quenching by a stratified flow in a hot horizontal pipe. Both phases were modeled using one-dimensional mass and momentum conservation equations. The wall temperature was computed using a 2-dimensional transient heat conduction equation. Their prediction for the wall temperature agreed well with their experimental results. Although significant progress was made in handling the momentum equations, the heat transfer correlations employed were not as advanced.

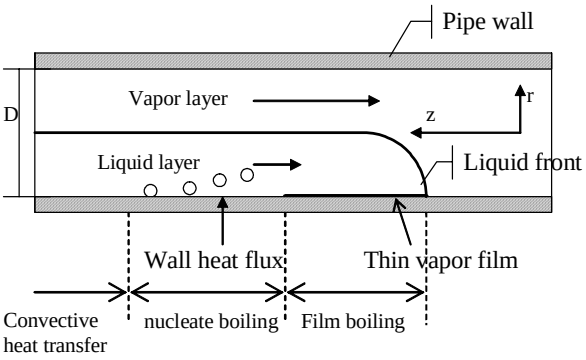

Fig. 1. Schematic of the chilldown heat transfer regimes in a horizontal pipe.

A typical chilldown process involves several heat transfer regimes as shown in Fig. 1. Near the liquid front is the film boiling. The knowledge of the heat transfer in the film boiling regime is relatively limited, because i) film boiling has not been the central interest in industrial applications; and ii) high temperature difference causes difficulties in experimental investigations. For the film boiling on vertical surfaces, early work was reported by Bromley [14], Dougall and Rohsenow [15] and Laverty and Rohsenow [16]. Film boiling in a horizontal cylinder was first studied by Bromley [17]; and the Bromley correlation was widely used. Breen and Westwater [18] modified Bromley's equation to account for very small tubes and large tubes. If the tube is larger than the wavelength associated with Taylor instability, the heat transfer correlation is reduced to Berenson's correlation [19] for a horizontal surface.

Empirical correlations for cryogenic film boiling were proposed by Hendrick et al. [20] [21], Ellerbrock et al. [22], von Glahn [23], Giarratano and Smith [24]. These correlations relate a simple or modified Nusselt number ratio to the Martinelli parameter. Giarratano and Smith [24] gave detailed assessment of these correlations. All these correlations are for steady state cryogenic film boiling. Their suitability for transient chilldown applications is questionable.

When the pipe wall chills down further, film boiling ceases and nucleate boiling occurs. It is usually assumed that the boiling switches from the film boiling to the nucleate boiling right away instead of passing through a transition boiling regime. The position of the film boiling transitioning to the nucleate boiling is often called rewetting front, because from that position the cold liquid starts touching the pipe wall. Usually the Leidenfrost temperature indicates the transition from the film boiling to the nucleate boiling.

Studies on forced convection boiling are extensive. A general correlation for saturated boiling was introduced by Chen [25]. Gungor and Winterton [26] modified Chen's correlation and extend it to subcooled boiling. Enhancement and suppression factors for macro-convective heat transfer were introduced. Gunger and Winterton's correlation can fit experimental data better than the modified Chen's correlation [27] and Stephan and Auracher correlation [28]. Kutateladze [29] and Steiner [30] also provided correlations for cryogenic fluids in pool boiling and forced convection boiling. Although they are not widely used, they are expected to be more applicable for cryogenic fluids since the correlation was directly based on cryogenic conditions. As the wall temperature drops further, boiling is suppressed and the heat transfer is governed by two-phase convection [31].

Although the two-fluid model can describe the fluid dynamics aspect of the chilldown process, it suffers from computational instability for moderately values of slip velocity between two phases, which limits its application. To gain the fundamental insight into the thermal interaction between the wall and the cryogenic fluid and to be able to rapidly predict chilldown in a long pipe, an alternative pseudo-steady model is developed. In this model, a liquid wave front speed is assumed to be constant and is the same as the bulk liquid speed [32]. It is also assumed that steady state thermal fields for both the liquid and the solid exist in a reference frame that is moving with the wave front. The heat transfer between the fluid and the wall is modeled using different heat transfer correlations depending on the operating heat transfer regime at a given location. Various improvements on the correlations are introduced, including the development of a new film boiling heat transfer model. The governing equation for the solid thermal field becomes a parabolic equation that can be efficiently solved. It must be emphasized that a great advantage of the pseudo-steady model is that one can assess the efficacy of the film boiling model independently from that of the nucleate boiling model since the down stream information in the nucleate boiling regime cannot affect the temperature in the film boiling regime. In other words, even if the nucleate boiling heat transfer coefficient is inadequate, the film boiling heat transfer coefficient can still be assessed in the film boiling regime by comparing with the measured temperature during the corresponding period. Once satisfactory performance is achieved for the film boiling regime, the nucleate boiling heat transfer model can be subsequently assessed. In the results section, those detailed assessments of the heat transfer coefficients are provided by comparing the computed temperature variations with the experimental measurements of Chung et al. [7]. Satisfactory results are obtained.

NOMENCLATURE

Bo	Boiling number
c	solid heat capacity
c_p	heat capacity
D	pipe diameter
d	thickness of pipe wall
g	gravity
h	heat transfer coefficient
h_{pool}	pool boiling heat transfer coefficient
h_{conv}	convection boiling heat transfer coefficient
h_{fg}	latent heat
Ja	Jacob number
k	thermal conductivity
k_{eff}	effective thermal conductivity
Nu	Nusselt number
p	pressure
R	radius of pipe
R_1 and R_2	inner and outer radius of pipe
Ra	Rayleigh number
Re	Reynolds number
Pc	Peclet number
Pr	Prandtl number
S	suppression factor
T	temperature
T_1	Leidenfrost temperature
T_2	transition temperature between nucleate boiling to convection heat transfer
T_o	room temperature
t	time
U	velocity
u and v	vapor film velocity
x and y	vapor film coordinates
Z	transformed coordinate
z, r, and φ	cylindrical coordinates
α	liquid volume fraction
χ_{tt}	Martinelli number
δ	vapor film thickness
ε	emissivity
ϕ	azimuthal coordinate
μ	viscosity
θ	dimensionless temperature;
σ	liquid surface tension; Stefan Boltzmann constant
Subscripts	
0	characteristic value
i and o	inner and outer pipe
l	liquid
v	vapor
w	wall
sat	saturated
Superscripts	
’	dimensionless variable

FORMULATION

In the pseudo-steady chilldown model, it is assumed that both the liquid and its wave front moves at a constant speed *U*. Thus the main emphasis of the present study is on the modeling of the heat transfer coefficients with stratified flow in the film boiling and forced convection boiling heat transfer regimes and the computation of the thermal field within the solid pipe. Comparisons are made with low Reynolds number data.

Solid Heat Transfer

The thermal field inside the solid wall is governed by the 3-dimensional unsteady energy equation:

$$\rho c\frac{\partial T}{\partial t}=\frac{\partial}{\partial z}\left(k\frac{\partial T}{\partial z}\right)+\frac{1}{r}\frac{\partial}{\partial r}\left(rk\frac{\partial T}{\partial r}\right)+\frac{1}{r}\frac{\partial}{\partial \varphi}\left(\frac{k}{r}\frac{\partial T}{\partial \varphi}\right) \quad (1)$$

Since the wave front speed *U* is assumed to be a constant, it can be expected that when the front is reasonably far from the entrance region of the pipe, the thermal field in the solid is in a steady state when it is viewed in the reference frame that moves with the wave front. Thus, the following coordinate transformation is introduced,

$$Z=z+Ut\,. \quad (2)$$

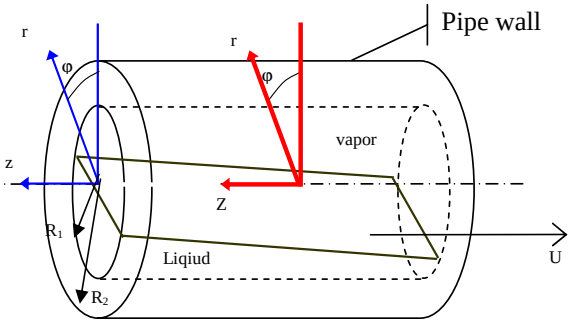

Fig. 2. Coordinate systems: laboratory frame is denoted by *z*; moving frame is denoted by *Z*.

Eq. (1) is then transformed to:

$$\rho cU\frac{\partial T}{\partial Z}=\frac{\partial}{\partial Z}\left(k\frac{\partial T}{\partial Z}\right)+\frac{1}{r}\frac{\partial}{\partial r}\left(rk\frac{\partial T}{\partial r}\right)+\frac{1}{r}\frac{\partial}{\partial \varphi}\left(\frac{k}{r}\frac{\partial T}{\partial \varphi}\right). \quad (3)$$

For further simplification, the following dimensionless parameters are introduced,

$$\theta=\frac{T-T_w}{T_w-T_{sat}},\ Z'=\frac{Z}{d},\ r'=\frac{r}{d},\ c'=\frac{c}{c_0},\ \text{and}\ k'=\frac{k}{k_0}\ , \quad (4)$$

where k_0 is the characteristic thermal conductivity, and c_0 is the characteristic heat capacity. Eq. (3) can be normalized as

$$Pc*c'\frac{\partial\theta}{\partial Z'}=\frac{\partial}{\partial Z'}\left(k'\frac{\partial\theta}{\partial Z'}\right)+\frac{1}{r'}\frac{\partial}{\partial r'}\left(r'k'\frac{\partial\theta}{\partial r'}\right)+\frac{1}{r'}\frac{\partial}{\partial\varphi}\left(\frac{k'}{r'}\frac{\partial\theta}{\varphi}\right), \quad (5)$$

where $Pc=\dfrac{\rho c_0 Ud}{k_0}$ is the Peclet number.

Under typical operating conditions for cryogenic chilldown, $Pc \sim O(10^2)$ - $O(10^3)$, the first term on the RHS of Eq. (5) is small compared with the rest of the terms and thus can be neglected. Eq. (5) becomes

$$Pc*c'\frac{\partial\theta}{\partial Z'}=\frac{1}{r'}\frac{\partial}{\partial r'}\left(r'k'\frac{\partial\theta}{\partial r'}\right)+\frac{1}{r'}\frac{\partial}{\partial\varphi}\left(\frac{k'}{r'}\frac{\partial\theta}{\varphi}\right), \quad (6)$$

which is parabolic. Hence in Z'-direction, only one condition is needed. In the φ-direction, periodic boundary conditions are used. On the inner and outer surfaces of the pipe wall, proper boundary conditions for the temperature are required.

For convenience, Z'=0 is set at the liquid wave front. In the region of Z'<0, the inner wall is exposed to the pure vapor. Although there may be some liquid droplets in the vapor that can cause evaporative cooling when the droplets deposit on the wall and the cold flowing vapor can absorb some heat from the wall, the heat flux due to these two mechanisms is small compared with the heat transfer between liquid and solid wall in the region of Z'>0. Hence, heat transfer for Z'<0 is neglected and it is assumed that $\theta = 1$ at $Z' = 0$. The computation starts from the Z'=0 to $Z' \to \infty$, until a steady state solution in the Z'-direction is reached. An implicit scheme in the Z'-direction is employed to solve Eq. (6).

Liquid and Vapor Flow

The two-phase flow is assumed to be stratified as was observed in [7]. Both liquid and vapor phases are assumed to be at the saturated state. The liquid volume fraction is used to determine the part of the wall in contact with the liquid or the vapor, and is specified at every cross-section along the Z'-direction based on experimental information. For the experimental conditions under consideration, visual studies [6] [7] show that the liquid volume fraction increases gradually, rather than abruptly, near the liquid wave front and becomes almost constant during most of the chilldown. Hence, the following liquid volume fraction variation is assumed as a function of time for the computation of the solid-fluid heat transfer coefficient,

$$\alpha = \alpha_0 \sin\left(\frac{t}{t_0} \cdot \frac{\pi}{2}\right) \qquad t < t_0, \tag{7}$$

$$\alpha = \alpha_0 \qquad t \geq t_0,$$

where t_0 is characteristic chilldown time, and α_0 is characteristic liquid volume fraction. Here the time when the nucleate boiling is almost suppressed and the slope of the wall temperature profile becomes flat is set as characteristic chilldown time. It is determined experimentally.

The vapor phase velocity is assumed to be a constant. However, it was not directly measured. It is computationally determined by trial-and-error by fitting the computed and measured wall temperature variations for numerous positions.

Heat Transfer Between the Cryogenic Fluid and Solid Pipe Wall

During cryogenic chilldown, the fluid in contact with the pipe wall is either liquid or vapor. The mechanisms of heat transfer between the liquid and the wall and between the vapor and the wall are different. Based on experimental measurements and theoretical analysis, liquid-solid heat transfer accounts for a majority of the total heat transfer. However, the prediction for the liquid-solid heat transfer is much more complicated than the heat transfer between the vapor and the wall. The heat transfer between the liquid and the wall is discussed first.

Heat Transfer between Liquid and Solid wall

The heat transfer between the liquid and the solid wall includes film boiling, nucleate boiling, and two-phase convective heat transfer. The transition from one type of boiling to another depends on many parameters, such as the wall temperature, the wall heat flux, and various properties of the fluid. For simplicity, a fixed temperature approach is adopted to determine the transition point. That is, if the wall temperature is higher than the Leidenfrost temperature, film boiling is assumed. If the wall temperature is between the Leidenfrost temperature and a transition temperature, T_2, nucleate boiling is assumed. If the wall temperature is below the transition temperature T_2, two-phase convection heat transfer is assumed. The values of the Leidenfrost temperature and the transition temperature are determined by matching the model prediction with the experimental results.

Film boiling heat transfer

Due to the high wall superheat encountered in the cryogenic chilldown, film boiling plays a major role in the heat transfer process in terms of the time span and in terms of the total amount of heat removed from the wall. Currently there exists no specific film boiling correlation for chilldown applications with such high superheat. If one uses conventional film boiling correlations, necessary modifications for cryogenic applications must be made for the chilldown.

A cryogenic film boiling heat transfer correlations was provided by Giarratano and Smith [24]

$$\left(\frac{Nu}{Nu_{calc}}\right) * Bo^{-0.4} = f(\chi_{tt}), \tag{8}$$

where Nu_{calc} is the Nusselt number for the two-phase convective heat transfer. In this correlation, the heat transfer coefficient is the averaged value for the whole cross section. Similar correlations for cryogenic film boiling also exist in the literature. The correlations were obtained from measurements conducted under steady state. The problem with the use of these steady state film boiling correlations is that they do not account for changes in flow regime. For example, for the same quality, the heat transfer rate for annular flow is much different from that for stratified flow. Available empirical correlations do not make such difference.

Furthermore, in this study, the local heat transfer coefficient is needed in order to incorporate the thermal interaction with the pipe wall. Since the two-phase flow regime information is available through visualization in the present study, the modeling effort needs to take into account the knowledge of the flow regimes.

There are several correlations for the film boiling based on the analysis of the vapor film boundary layer and the stability of the thin vapor film, such as Bromley's correlation [17] and Breen and Westerwater's correlation [18] for film boiling on the outer surface of a hot tube. Frederking and Clark's [33] and Carey's [34] correlations, for the film boiling on the surface of a sphere, are included as well. However, none of these was obtained for cryogenic fluids or for film boiling on the inner surface of a pipe or tube.

A new correlation for cryogenic film boiling inside a tube is presented here. The schematic diagram of the film boiling inside a pipe is shown in Fig. 3 with a cross-sectional view. The bulk liquid is near the bottom of the pipe. Beneath the liquid is a thin vapor film. Due to the buoyancy force, the vapor in the

film flows upward along the azimuthal direction. Heat is transferred through the thin vapor film from the solid to the liquid. Reliable heat transfer correlation for film boiling in pipes or tubes requires knowledge of the thin vapor film thickness, which can be obtained by solving the film layer continuity, momentum, and energy equations.

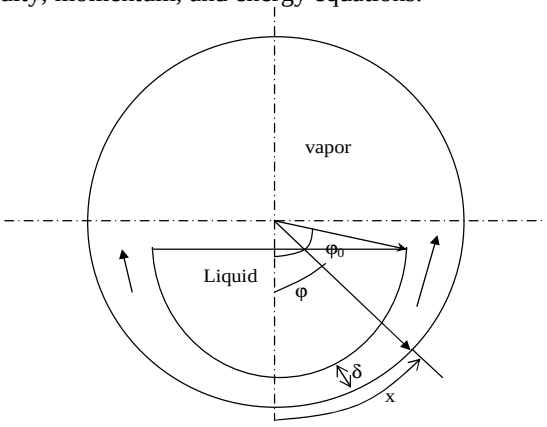

Fig. 3. Schematic diagram of film boiling in stratified flow in a pipe [13] [34].

To simplify the analysis for vapor film heat transfer, it is assumed the liquid velocity in the azimuthal direction is zero and the vapor flow in the direction perpendicular to the cross-section is negligible. It is further assumed that the vapor film thickness is small compared with the pipe radius and the vapor flow is quasi-steady, incompressible and laminar. The laminar flow assumption can be confirmed *post priori* as the Reynolds number, *Re*, based on the film velocity and film thickness is typically of $O(10^0 \sim 10^2)$. In terms of the *x*- & *y*-coordinates and (*u*, *v*) velocity components shown in Fig. 3, the governing equations for the vapor flow are similar to boundary-layer equations:

$$\frac{\partial u}{\partial x}+\frac{\partial v}{\partial y}=0, \tag{9}$$

$$u\frac{\partial u}{\partial x}+v\frac{\partial u}{\partial y}=-\frac{1}{\rho_v}\frac{\partial p}{\partial x}+\nu_v\frac{\partial^2 u}{\partial y^2}-g\sin\varphi, \tag{10}$$

$$u\frac{\partial T}{\partial x}+v\frac{\partial T}{\partial y}=\alpha_v\frac{\partial^2 T}{\partial y^2}, \tag{11}$$

where subscript *v* refers to the properties of vapor.

Because the length scale in the azimuthal (*x*) direction is much larger than the length scale at the normal (*y*) direction, the *v*-component may be neglected. Furthermore, the convection term is assumed small and is neglected. The resulting momentum equation is simplified to

$$\frac{1}{\rho_v}\frac{\partial p}{\partial x}=\nu_v\frac{\partial^2 u}{\partial y^2}-g\sin\varphi. \tag{12}$$

The vapor pressure can be evaluated by considering the hydrostatic pressure from liquid core as:

$$p=p_0+\rho_l gR\left(\cos\left(\frac{x}{R}\right)-\cos\varphi_0\right), \tag{13}$$

where φ_0 is the angular position where the film merges with the vapor core. The momentum equation becomes

$$\frac{(\rho_l-\rho_v)}{\rho_v}g\sin\left(\frac{x}{R}\right)+\nu_v\frac{\partial^2 u}{\partial y^2}=0. \tag{14}$$

The vapor velocity boundary condition is $u=0$ at $y=0$ and $u=u_l=0$ at $y=\delta$. The vapor velocity profile is:

$$u=\frac{(\rho_l-\rho_v)}{2\nu_v\rho_v}g\sin\left(\frac{x}{R}\right)*\left(\delta y-y^2\right). \tag{15}$$

The mean velocity $\bar{u}$ is

$$\bar{u}=\frac{1}{\delta}\int_0^\delta u dy=\frac{(\rho_l-\rho_v)\delta^2 g}{12\nu_v\rho_v}\sin\left(\frac{x}{R}\right). \tag{16}$$

The energy and mass balances on the vapor film requires that

$$\frac{k_v}{h_{fg}}dx*\left[-\left(\frac{\partial T}{\partial y}\right)_{y=\delta}\right]=d\dot{m}=\rho_v d(\bar{u}\delta). \tag{17}$$

Neglecting the convection, the vapor energy equation is:

$$\frac{\partial^2 T}{\partial y^2}=0. \tag{18}$$

The following linear temperature profile is thus obtained,

$$\frac{T-T_{sat}}{T_w-T_{sat}}=1-\frac{y}{\delta}. \tag{19}$$

Substituting the temperature and velocity profiles into Eq. (17) yields

$$\frac{\delta}{R}\frac{d}{d\theta}\left(\left(\frac{\delta}{R}\right)\sin\varphi\right)=\frac{12k_v\nu_v}{h_{fg}(\rho_l-\rho_v)gR^3}(T_w-T_{sat}). \tag{20}$$

Eq. (20) has an analytical solution:

$$\frac{\delta}{R}=2\left(\frac{6Ja}{Ra}\right)^{\frac{1}{4}}F(\varphi), \tag{21}$$

where *Ja* is Jacob number and *Ra* is Raleigh number:

$$Ja=\frac{c_{p,v}(T_w-T_{sat})}{h_{fg}}, \tag{22}$$

$$Ra=\frac{gD^3(\rho_l-\rho_v)}{\nu_v\alpha_v\rho_v}, \tag{23}$$

and $F(\varphi)$

$$F(\varphi)=\left(\frac{\frac{4}{3}\int_0^\varphi \sin^{1/3}\varphi' d\varphi'}{\sin^{0.75}\varphi}\right)^{\frac{1}{4}}, \tag{24}$$

describes the geometric dependence of the vapor film thickness.

The mean velocity $\bar{u}$ as a function of φ is thus

$$\bar{u}=\left(\frac{(T_w-T_{sat})(\rho_l-\rho_v)gR}{12\nu_v\rho_v^2 h_{fg}}\right)^{\frac{1}{2}}F^2(\varphi)\sin(\varphi). \tag{25}$$

Curves for $F(\varphi)$ and $F^2(\varphi)\sin\varphi$ based on the numerical integration are shown in Fig. 4. The vapor film thickness has a minimum at $\varphi=0$ and is nearly constant for $\varphi<\pi/2$. It rapidly grows after $\varphi>\pi/2$. The singularity at the top of tube when $\varphi\to\pi$ is of no practical significance since the film will merge with the vapor core at the vapor-liquid interface. The

vapor velocity is controlled by $F(\varphi)^2 \sin\varphi$ which is zero at the bottom of the pipe and increases almost linearly in the lower part of the tube where the vapor film thickness does not change substantially. In the upper part of the tube, due to the increase in the vapor film thickness, the vapor velocity gradually drops back to zero at the top of the tube. Thus a maximum velocity may exist in the upper part of the tube.

The local film boiling heat transfer coefficient is easily obtained from the linear temperature profile. It is

$$h = \frac{k_v}{\delta} = 0.6389 \frac{k_v}{DF(\varphi)} \left(\frac{Ra}{Ja} \right)^{\frac{1}{4}}. \quad (25)$$

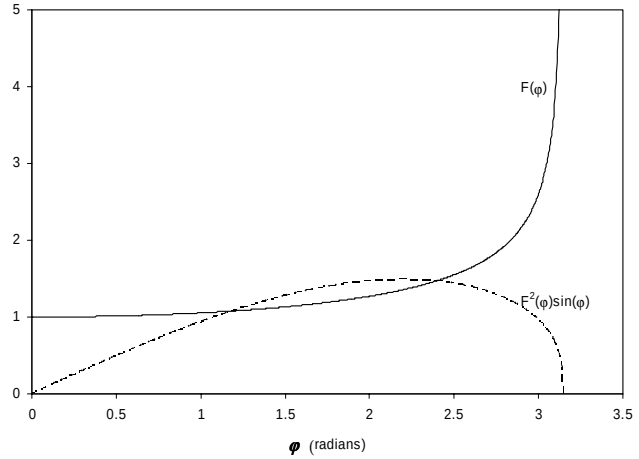

Fig. 4. Numerical solutions of the vapor thickness and velocity influence functions.

Forced convection boiling and two-phase convective heat transfer

For the flow boiling heat transfer, Gungor and Winterton's correlation [26] is widely used due to its good agreement with a large data set. However, a closer examination on this correlation shows that it is based mainly on the following parameters: *Pr*, *Re*, and quality *x*. Similar to the development of conventional film boiling correlations, these parameters all reflect overall properties of the flow in the pipe and are not directly related to flow regimes. Thus it cannot be used to predict the local heat transfer coefficients applied in chilldown.

Chen's [25] flow boiling correlation is based on separating the heat transfer into micro- and macro-convection components of heat transfer. The micro-convection heat transfer represents the contribution from ebullition, and the macro-convection represents the contribution from the forced convection heat transfer. However his correlation fits best for annular flow since it was developed for vertical flows. For the stratified flow regime, Chen's correlation may not be applicable.

Several correlations have been attempted with this study, including Gungor and Winterton's correlation [26], Chen's correlation [25], and Kutateladze's correlation [29]. None of them gives a satisfactory heat transfer rate that is needed to match the experimentally measured temperature histories in [7] for the forced convection boiling regime. Among them, Kutateladze correlation gives more reasonable results. In this correlation, the total heat transfer coefficient *h* is

$$h = h_{conv} + h_{pool}, \quad (26)$$

where h_{conv} is given by the Dittus-Boelter equation for fully developed pipe flow,

$$h_{conv} = 0.023 * \mathrm{Re}_l^{0.8} \, \mathrm{Pr}_l^{0.4} \, k_l / D_l \quad (27)$$

where Re_l is defined with liquid hydraulic diameter D_l, and the pool nucleated boiling heat transfer coefficient h_{pool} is

$$h_{pool} = 0.487 * 10^{-10} * \left[\frac{k_l \rho_l^{1.282} \, p^{1.750} \left(c_{p,l} \right)^{1.5}}{\left(h_{fg} \rho_v \right)^{1.5} \sigma^{0.906} \mu_l^{0.626}} \right] \Delta T^{1.5}, \quad (28)$$

in which ΔT is the wall superheat.

Kutateladze correlation [29] was proposed without considering the effect of nucleation site suppression. This obviously leads to an overestimation of the nucleate boiling heat transfer rate. Hence a modified version of Kutateladze correlation, Eq. (29), is used,

$$h = h_{conv} + S * h_{pool}, \quad (29)$$

with *S* being the suppression factor and h_{pool} is given by Eq. (28).

When ΔT drops to a certain range all the nucleate sites are suppressed. The heat transfer is dominated by two-phase forced convection. The heat transfer coefficient can then be predicated using Eq. (27), when the flow is turbulent, or Eq. (30), when the flow is laminar.

$$h_{conv} = 4.36 * k_l / D_l. \quad (30)$$

Heat Transfer between Vapor and Solid Wall

The heat transfer between the vapor and the wall can be estimated by treating the flow as a fully developed convection flow, neglecting the liquid droplets that are entrapped in the vapor. The heat transfer coefficient of the vapor forced convection flow is

$$h_v = 0.023 * \mathrm{Re}_v^{0.8} \, \mathrm{Pr}_v^{0.4} \, k_v / D_v \quad \text{(turbulent flow)} \quad (31)$$

or

$$h_v = 4.36 * k_v / D_v \quad \text{(laminar flow)} \quad (32)$$

where Re_v is defined with vapor phase hydraulic diameter D_v.

Heat Transfer between Solid Wall and Environment

For a cryogenic flow facility, although serious insulation is applied, the heat leakage to the environment is still considerable due to the large temperature difference between the cryogenic fluid and the environment. It is necessary to evaluate the heat leakage from the inner pipe to environment in order to make a realistic assessment of the model prediction with the experimental data [7].

A vacuum insulation chamber between the inner and outer pipes is used in the cryogenic transport pipe [7], as shown in Fig. 5. Radiation heat transfer exists between the inner and outer pipe. Furthermore, the space between the inner and outer pipe is not an absolute vacuum. There is residual air that causes the free convection between the inner and outer pipe driven by the temperature difference of the inner and outer pipe.

The radiation between the inner pipe and outer pipe becomes significant when the inner pipe is chilled down. The heat transfer coefficient is proportional to the difference of the fourth power of wall temperatures. Exact evaluation of the radiation heat transfer between the inner and outer pipe is a

difficult task. Hence a simplified model based on the overall radiation heat transfer between long concentric cylinders with a constant temperature at the inner and outer pipes [31] is used to evaluate the heat transfer rate at every axial location of the pipe. It is not quantitatively correct, but can provide reasonable estimates for the magnitude of the radiation heat transfer between the pipes through the vacuum. The local radiation heat transfer rate per unit area on the surface of inner pipe q'_{rad} is

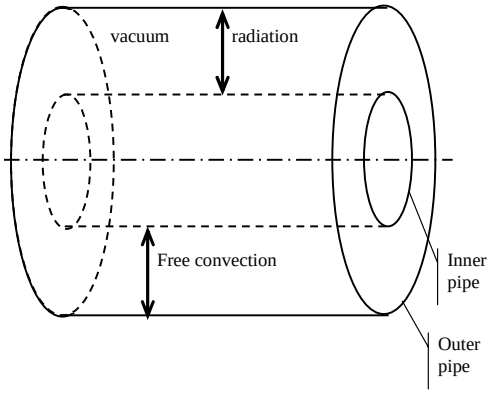

Fig. 5. Schematic of vacuum insulation chamber.

$$q'_{rad} = \frac{\sigma(T_{wall}^4 - T_o^4)}{\frac{1}{\varepsilon_i} + \frac{1-\varepsilon_o}{\varepsilon_o}\left(\frac{r_i}{r_o}\right)}, \quad (33)$$

where σ is the Stefan Boltzmann constant, (r_i, ε_i) and (r_o, ε_o) are the radius and emissivity of inner pipe and outer pipe, respectively, and T_{wall} is the local inner wall temperature, T_o is the room temperature that is assumed constant in the entire outer pipe. Here the emissivity is also assumed to be constant during the entire chilldown process.

For the free convection heat transfer due to the residual air in the vacuum chamber between the inner pipe and outer pipe, Raithby and Hollands' correlation [35] is used for the heat transfer rate. The average heat transfer rate per unit length of the cylinder is

$$q'_{frc} = \frac{2\pi k_{eff}}{\ln(r_o/r_i)}(T_i - T_o), \quad (34)$$

where T is assumed constant on the inner and outer wall along the azimuthal direction, and k_{eff} is the effective thermal conductivity. Detailed evaluation of k_{eff} is shown in [35].

RESULTS AND DISCUSSIONS

In the experiment by Chung et al. [7], liquid nitrogen was used as the cryogen. The flow regime is revealed to be the stratified flow by visual observations, as shown in Fig. 7, and the wall temperature history in several azimuthal positions is measured by imbedded thermocouples.

Experiment of Chung et al.

In the experiment by Chung et al. [7], a concentric pipe test section (Fig. 6) was used. The chamber between the inner and outer pipe is vacuum, sealed but about 20% air remained. The inner diameter (I.D.) and outer diameter (O.D.) of the inner pipe are 11.1 and 15.9 mm, and I.D. and O.D. of the outer pipe are 95.3 and 101.6mm, respectively. Numerous thermocouples were placed at different locations of the inner pipe. Some were embedded very close to the inner surface of the inner pipe while others measure the outside wall temperature of the inner pipe. Experiments were carried out at room temperature and atmospheric pressure. Liquid nitrogen flows from a reservoir to the test section driven by gravity. As the liquid nitrogen flows through the pipe, it evaporates and chills the pipe. Fig.7 shows the pictures of nitrogen flow in the pipe at t=0.6s, t=15.8s, t=33.2s, and t=94.93s. The flow is from right to the left. Obviously, the flow is stratified. The nitrogen mass flux is around 3.7E-4 kg/s and the measured average liquid nitrogen velocity is U~5 cm/s. Details of the experiment facility and results can be found in Chung et al. [7]. The vapor velocity is not measured in the experiment. In this study, it is determined through trial-and-error by fitting the computed and measured temperature histories. The characteristic liquid volume fraction is 0.3 from the recorded video images. The characteristic time used in this computation is $t_0 = 100s$. The Leidenfrost temperature for the nitrogen is around 180 K from experimental results [6][7]; hence the temperature when the film boiling ends and nucleate boiling starts is set at 180 K. The transition temperature at which purely two-phase convection heat transfer begins is 140 K based on experimental results. The material of the inner pipe and outer pipe used in the experiment of [7] are Pyrex glass with emissivity of 0.82 (based on room temperature).

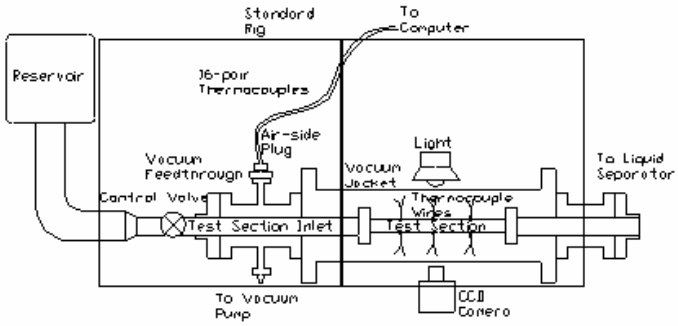

Fig. 6. Schematic of Chung et al.'s cryogenic two-phase flow test apparatus [7].

Comparison of Pipe Wall Temperature

In the computation, there are 40 grids along the radial direction and 40 grids along the azimuthal direction for the inner pipe (Fig. 8). The results of the temperature profile at 40X40 grids and the higher grid resolution shows that 40X40 grids are sufficient. Figures 9-10 compare the measured and computed wall temperature as a function of time at positions 11, 12, 14 and 15 shown in Fig. 8. For the modified Kutateladze correlation a proper suppression factor of 0.01 is obtained by best fit. The small suppression is supported by the visual observation that the majority of nucleate sites are suppressed in cryogenic chilldown. The vapor velocity is 0.5m/s based on the best fit. The overall temperature histories agree well in the film boiling stage. Thus, the film boiling heat transfer coefficient based on a first principles approach and the incorporated flow structure gives a very good prediction. It

must also be noted that the value of the Leidenfrost temperature does not affect the computed temperature history prior to the transition point since the governing equation is parabolic. The good agreement before the Leidenfrost temperature is reached is entirely due to the excellent performance of the new film boiling heat transfer coefficient.

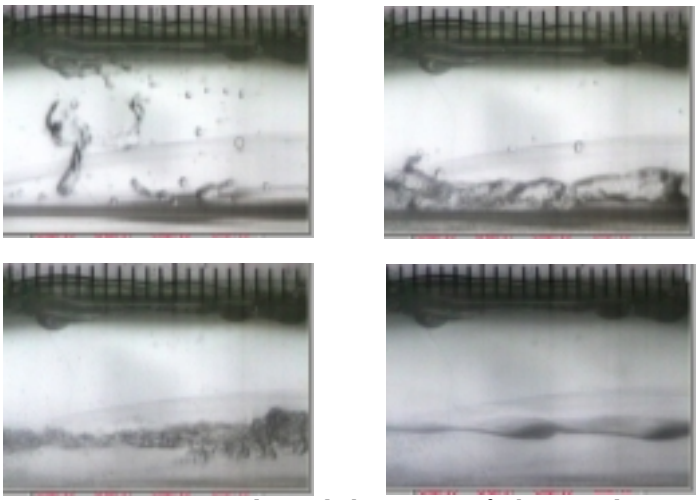

Fig. 7. Experimental visual observation of Chung et al.'s cryogenic two-phase flow experiment [7].

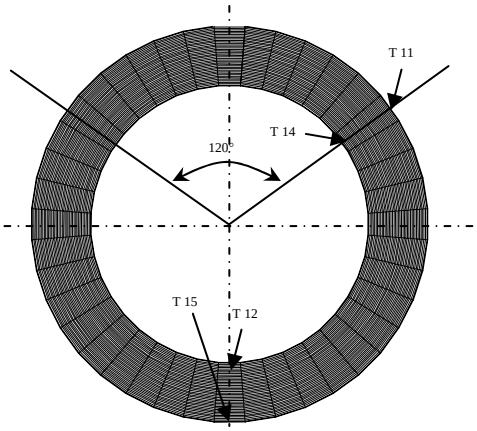

Fig. 8. Computational grid arrangement and position of thermocouples.

During the stage of the rapidly decreasing wall temperature after the Leidenfrost temperature, the computed wall temperature drops slightly faster than the measured value. The rapid decrease in the wall temperature is due to initiation of nucleate boiling which is significantly more efficient for heat transfer than film boiling. Reasonable agreement between the computed and measured histories in this nucleate boiling regime is due to: i) the good agreement already achieved in the film boiling stage; ii) valid choice for the Leidenfrost temperature that switches the heat transfer regime correctly; and iii) appropriate modification of Kutateladze correlations.

In the final stage of chilldown, the wall temperature decreases slowly, and the computed wall temperature shows the same trend as the measured one but tends to be a little lower. Fig. 11 shows the temperature distribution of a given cross-section at different times during chilldown. Because the upper part of pipe wall is exposed to the nitrogen vapor, the cooling effect is much reduced.

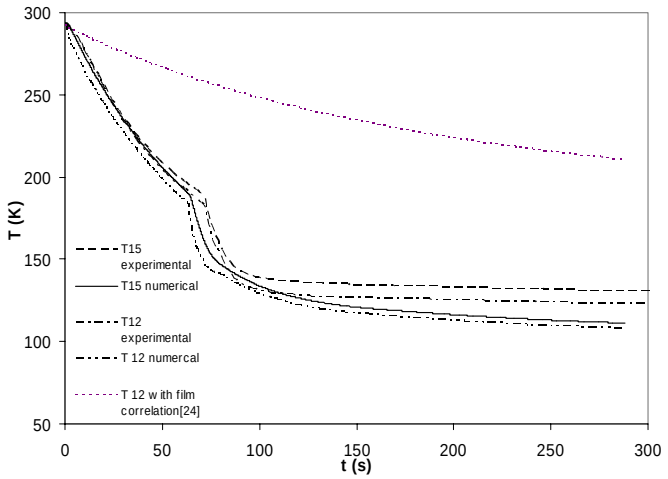

Fig. 9. Comparison between measured and predicted transient wall temperatures of positions 12 and 15, which is at the bottom of pipe.

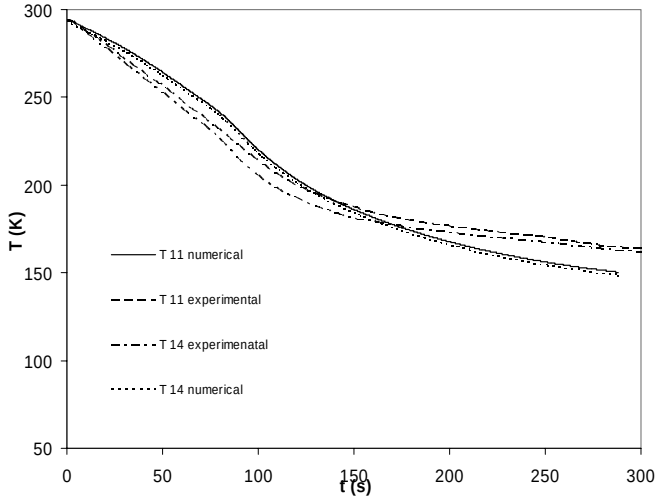

Fig. 10. Comparison between measured and predicted transient wall temperatures of positions 11 and 14, which is at the bottom of pipe.

Discussions and Remarks

In Fig. 9, the wall temperature based on the film boiling correlation of Giarratano and Smith [24] is also shown. Apparently, the correlation of Giarratano and Smith [24] gives a very low heat transfer rate so that the wall temperature remains high. This comparison confirms our earlier argument that correlations based on the overall flow parameter, such as quality and averaged Reynolds number, are not applicable for the simulation of the unsteady chilldown.

The nucleate flow boiling correlations of Gungor and Winterton [26], Chen [25], and Kutateladze [29] are also compared in this study. Gungor and Winterton's correlation fails to give a converged heat transfer rate during the transition from film boiling to nucleate boiling. Chen's correlation

overestimates the heat transfer rate, and causes an unrealistically large temperature drop on the wall, which results in the halt of the computation. Only Kutateladze correlation gives an acceptable heat transfer rate. However, the temperature drop near the bottom of the pipe is still faster than the measured one as shown in Fig. 9. This may be due to the fact that most of nucleate boiling correlations were obtained from experiments of low wall superheat. However, in cryogenic chilldown, the wall superheat is much higher than that in normal nucleate boiling experiments. Another reason is that the original Kutateladze correlation does not include a suppression factor. This leads to overestimating the heat transfer coefficient. The modified correlation with the suppression factor gives reasonable chilldown results in Fig. 9. Although this modified Kutateladze nucleate boiling correlation is not a reliable correlation due to experimental specified factors, it is still useful because of qualitatively capturing the nucleate boiling heat transfer in cryogenic chilldown.

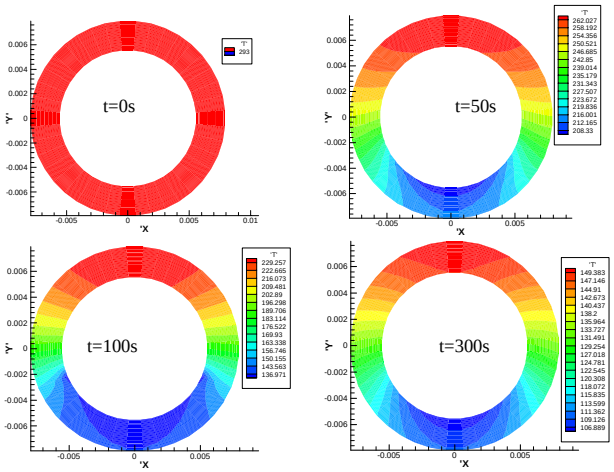

Fig. 11. Cross section wall temperature distribution at t=0, 50, 100 and 300 seconds.

Further examination of Figs. 9 and 10 indicates that although we have considered the heat leak from the outer wall to the inner wall through radiation and free convection, the computed temperature is still lower than the measured temperature during the final stage of chilldown. In this final stage the heat transfer rate between the fluid and the wall is low due to the lower wall superheat. The temperature difference between the computed and measured values at positions 12 and 15 suggests that there may be additional heat loss, which affects the measurements but is not taken in account in the present modeling.

In this study, pseudo-steady chilldown model is developed to predict the chilldown process in a horizontal pipe in the stratified flow regime. This model can also be extended to describe the annular flow chilldown in the horizontal or the vertical pipe with minor changes on the boundary condition for the solid temperature. It can also be extended to study the chilldown in the slug flow as long as we specify the contact period between the solid and the liquid or the vapor. The disadvantage of the current pseudo-steady chilldown model is that the fluid interaction inside the pipe is largely neglected and both the vapor and liquid velocities are assumed to be constant. Compared with a more complete model that incorporates the two-fluid model, the present pseudo-steady chilldown model requires more experimental measurements as inputs. However, the pseudo-steady chilldown model is computationally more robust and efficient for predicting chilldown. Overall, it provides reasonable results for the solid wall temperature. While a more complete model for chilldown that incorporates the mass, momentum, and energy equations of the vapor and the liquid is being developed to reduce the dependence of the experimental inputs for the liquid velocity and trial-and-error for the vapor velocity, the present study has revealed useful insight into the key elements of the two-phase heat transfer encountered in the chilldown process which have been largely ignored. It also provides the necessary modeling foundation for incorporating the two-fluid model.

CONCLUSIONS

A pseudo-steady chilldown computational model has been developed to understand the heat transfer mechanisms of cryogenic chilldown and predict the chilldown wall temperature history in a horizontal pipeline. The model assumes a constant speed of the moving liquid wave front, and a steady thermal field in the solid within a moving frame of reference. This allows the 3-dimensional unsteady problem to be transformed to a 2-dimensional, parabolic problem. A new film boiling heat transfer coefficient for cryogenic chilldown has been developed using first principles and incorporating the stratified flow structure. The new film boiling coefficient is also successfully implemented by Jackson et al. [36]. The existing nucleate boiling heat transfer correlations may not work well for cryogenic conditions. A modified Kutateladze correlation with the suppression factor adequately describes the nucleate boiling heat transfer coefficient. With the new and modified heat transfer correlations, the pipe wall temperature history based on the pseudo-steady chilldown model matches well with the experimental results by Chung et al. [7] for almost the entire chilldown process. The pseudo-steady chilldown model has captured the important features of the thermal interaction between the pipe wall and the cryogenic fluid.

ACKNOWLEDGMENTS

This Work was supported by NASA Glenn Research Center under contract (NAG3-2750) and NASA Kennedy Space Center.

REFERENCES

1. Burke, J.C., Byrnes, W.R., Post, A.H., and Ruccia, F.E., 1960, “Pressure Cooldown of Cryogenic Transfer Lines”, Advances in Cryogenic Engineering, **4**, pp. 378-394.
2. Graham, R.W., Hendricks, R.C., Hsu, Y.Y., and Friedman, R., 1961, “Experimental Heat Transfer and Pressure Drop of Film Boiling Liquid Hydrogen Flowing through A Heated Tube”, Advances in Cryogenic Engineering, **6**, pp. 517-524.
3. Bronson, J.C., Edeskuty, F.J., Fretwell, J.H., Hammel, E.F., Keller, W.E., Meier, K.L., Schuch, and A.F, Willis, W.L., 1962, “Problems in Cool-Down of Cryogenic Systems”, Advances in Cryogenic Engineering, **7**, pp. 198-205.
4. Chi, J.W.H., and Vetere, A.M., 1963, “Two-Phase Flow During Transient Boiling of Hydrogen and Determination

of Nonequilibrium Vapor Fractions", Advances in Cryogenic Engineering, **9**, pp. 243-253.
5. Steward, W.G., Smith and R. V., Brennan, J.A., 1970, "Cooldown Transients in Cryogenic Transfer Lines", Advances in Cryogenic Engineering, **15**, pp. 354-363.
6. Velat, C., Jackson, J., Klausner, J.F., and Mei, R., 2004, "Cryogenic Two-Phase Flow during Chilldown," Proceedings of the ASME HT-FED Conference, Charlotte.
7. Chung, J. N., Yuan, K., and Xiong, R., 2004, "Two-Phase Flow and Heat Transfer of a Cryogenic Fluid during Pipe Chilldown", Proceedings of 5th International Conference on Multiphase Flow, Yokohama, Japan, pp. 468.
8. Martinelli, R.C., and Nelson, D.B., 1948, "Prediction of Pressure Drop During Forced –Circulation Boiling of Water", Transaction of ASME, **70**, pp. 695-701.
9. Chi, J.W.H., 1965, "Cooldown Temperatures and Cooldown Time During Mist Flow", Advances in Cryogenic Engineering, **10**, pp. 330-340.
10. Cross, M.F., Majumdar, A.K., Bennett Jr., and J.C., Malla, R. B., 2002, "Model of chilldown in Cryogenic Transfer Linear", Journal of Spacecraft and Rockets, **39**, pp. 284-289.
11. Chan, A. M. C., and Banerjee, S., 1981, "Refilling and Rewetting of a Hot Horizontal Tube part I: Experiment", Journal of Heat Transfer, **103**, pp. 281-286.
12. Chan, A. M. C., and Banerjee, S., 1981, "Refilling and Rewetting of a Hot Horizontal Tube part II: Structure of a Two-Fluid Model", Journal of Heat Transfer, **103**, pp. 287-292.
13. Chan, A. M. C., and Banerjee, S., 1981, "Refilling and Rewetting of a Hot Horizontal Tube part III: Application of a Two-Fluid Model to Analyze Rewetting", Journal of Heat Transfer, **103**, pp. 653-659.
14. Bromley, J. A., 1950, "Heat Transfer in Stable Film Boiling", Chemical Engineering Progress, **46**, No.5, pp. 221-227.
15. Dougall, R.S., Rohsenow, W. M., 1963, "Film boiling on the inside of vertical tubes with upward flow of the fluid at low qualities", MIT report no 9079-26, MIT.
16. Laverty, W.F., and Rohsenow, W.M., 1967, "Film Boiling of saturated Nitrogen Flowing in a Vertical Tube", Journal of Heat transfer, **89**, pp. 90-98.
17. Bromley, J. A., 1950, "Heat Transfer in Stable Film Boiling", Chemical Engineering Progress, **46**, No.5, pp. 221-227.
18. Breen, B.P., and Westwater, J.W., 1962, "Effect if Diameter of Horizontal Tubes on Film Heat Transfer", Chemical Engineering Progress, **58**, no.7, pp. 67.
19. Berenson, P.J., 1961, "Film-Boiling Heat Transfer from a Horizontal Surface", Journal of Heat Transfer, **83**, pp. 351-358.
20. Hendricks, R. C., Graham, R. W., Hsu, Y. Y., and Friedman, R., 1961, "Experimental Heat Transfer and Pressure Drop of Liquid Hydrogen Flowing Through a Heated Tube", NAS TN D-765.
21. Hendricks, R. C., Graham, R. W., Hsu, Y. Y., and Friedman, R., 1966, "Experimental Heat Transfer Results for Cryogenic Hydrogen Flowing in Tubes at Subcritical and Supercritical Pressure to 800 pounds per Square Inch Absolute", NASA TN D-3095.
22. Ellerbrock, H.H., Livingood, J. N. B., and Straight, D. M., 1962, "Fluid-Flow and Heat-Transfer Problems in Nuclear Rockets", NASA SP-20.
23. von Glahn, U. H., 1964, "A Correlation of Film-Boiling Heat Transfer Coefficients Obtained with Hydrogen", Nitrogen and Freon 113 in Forced Flow, NASA TN D-2294.
24. Giarratano, P. J., Smith, R. V., 1965, "Comparative study of Forced Convection Boiling Heat Transfer Correlations for Cryogenic Fluids", Advances in Cryogenic Engineering, **11**, pp. 492-505.
25. Chen, J. C., 1966, "Correlation for Boiling Heat Transfer to Saturated Fluids in Convective Flow", Industry Engineering Chemistry Process Design and Development, **5**, pp. 322-329.
26. Gungor, K. E., Winterton, R. H. S., 1996, "A General Correlation for Flow Boiling in Tubes and Annuli", International Journal of Heat Mass Transfer, **29**, No.3, pp. 351-358.
27. Bennett, D. L., and Chen, J. C., 1980, "Forced Convection for the in Vertical Tubes for Saturated Pure Components and Binary Mixture", A.I.Ch.E. Journal, **26**, pp. 454-461.
28. Stephan, K., and Auracher, H., 1981, "Correlation for Nucleate Boling Heat Transfer in Forced convection", International Journal of Heat Mass Transfer, **24**, pp.99-107.
29. Kutateladze, S.S., 1952, "Heat Transfer in Condensation and Boiling", Atomic Energy Commission Translation 3770, Tech. Info. Service, Oak Ridge, Tennessee.
30. Steiner, D., May 1986, "Heat Transfer During Flow Boiling of Cryogenic Fluids in Vertical and Horizontal Tubes", Cryogenics, **26**, pp. 309-318.
31. Incropera, F.P., Dewitt, D.P., 2002, Fundamentals of Heat and Mass Transfer, 5th edition, John Willey& Sons.
32. Thompson, T. S., 1972, "An Analysis of the Wet-Side Heat-Transfer Coefficient during Rewetting of a Hot Dry Patch", Nuclear Engineering and Design, **22**, pp. 212-224.
33. Ferderking, T.H.K., and Clark, J.A., 1963, "Nature Convection Film Boling on A Sphere", Advanced Cryogenic Engineering, **8**, pp. 501-506.
34. Carey, V. P., 1992, Liquid-Vapor Phase-Change Phenomena, Taylor & Francis Press.
35. Raithby, G.D., and Hollands, K.G.T., 1975, "A General Method of Obtaining Approximate Solutions to Laminar and Turbulent Free Convection Problems", Advances in Heat Transfer , **11**, pp.265-315 Academic Press, New York.
36. Jackson, J., Liao, J., Klausner, J.F., and Mei, R., 2005, "Transient Heat Transfer during Cryogenic Chilldown", ASME Summer Heat Transfer Conference, San Francisco.

